Journal for ImmunoTherapy of Cancer

Single-cell transcriptomics identifies pathogenic T-helper 17.1 cells and pro-inflammatory monocytes in immune checkpoint inhibitor-related pneumonitis

Amelie Franken ,[1] Pierre Van Mol,[1,2] Sam Vanmassenhove,[1] Elena Donders,[1,2] Rogier Schepers,[1] Thomas Van Brussel,[1] Christophe Dooms,[2,3] Jonas Yserbyt,[4] Nico De Crem,[4] Dries Testelmans,[3,4] Walter De Wever,[5] Kristiaan Nackaerts,[2,3] Johan Vansteenkiste,[2,3] Robin Vos,[3,4] Stéphanie Humblet-Baron,[6] Diether Lambrechts,[1] Els Wauters [2,3]

To cite: Franken A, Van Mol P, Vanmassenhove S, *et al*. Single-cell transcriptomics identifies pathogenic T-helper 17.1 cells and pro-inflammatory monocytes in immune checkpoint inhibitor-related pneumonitis. *Journal for ImmunoTherapy of Cancer* 2022;**10**:e005323. doi:10.1136/jitc-2022-005323

► Additional supplemental material is published online only. To view, please visit the journal online (http://dx.doi.org/10.1136/jitc-2022-005323).

AF and PVM contributed equally. DL and EW contributed equally.

Accepted 13 September 2022

For numbered affiliations see end of article.

Correspondence to
Professor Diether Lambrechts; diether.lambrechts@kuleuven.be

ABSTRACT

Background Immune checkpoint inhibitor (ICI)-related pneumonitis is the most frequent fatal immune-related adverse event associated with programmed cell death protein-1/programmed death ligand-1 blockade. The pathophysiology however remains largely unknown, owing to limited and contradictory findings in existing literature pointing at either T-helper 1 or T-helper 17-mediated autoimmunity. In this study, we aimed to gain novel insights into the mechanisms of ICI-related pneumonitis, thereby identifying potential therapeutic targets.

Methods In this prospective observational study, single-cell RNA and T-cell receptor sequencing was performed on bronchoalveolar lavage fluid of 11 patients with ICI-related pneumonitis and 6 demographically-matched patients with cancer without ICI-related pneumonitis. Single-cell transcriptomic immunophenotyping and cell fate mapping coupled to T-cell receptor repertoire analyses were performed.

Results We observed enrichment of both CD4+ and CD8+ T cells in ICI-pneumonitis bronchoalveolar lavage fluid. The CD4+ T-cell compartment showed an increase of pathogenic T-helper 17.1 cells, characterized by high co-expression of *TBX21* (encoding T-bet) and RORC (ROR-γ), *IFN-G* (IFN-γ), *IL-17A*, *CSF2* (GM-CSF), and cytotoxicity genes. Type 1 regulatory T cells and naïve-like CD4+ T cells were also enriched. Within the CD8+ T-cell compartment, mainly effector memory T cells were increased. Correspondingly, myeloid cells in ICI-pneumonitis bronchoalveolar lavage fluid were relatively depleted of anti-inflammatory resident alveolar macrophages while pro-inflammatory 'M1-like' monocytes (expressing *TNF*, *IL-1B*, *IL-6*, *IL-23A,* and GM-CSF receptor *CSF2RA, CSF2RB*) were enriched compared with control samples. Importantly, a feedforward loop, in which GM-CSF production by pathogenic T-helper 17.1 cells promotes tissue inflammation and IL-23 production by pro-inflammatory monocytes and vice versa, has been well characterized in multiple autoimmune disorders but has never been identified in ICI-related pneumonitis.

Conclusions Using single-cell transcriptomics, we identified accumulation of pathogenic T-helper 17.1 cells in ICI-pneumonitis bronchoalveolar lavage fluid—a phenotype explaining previous divergent findings on T-helper 1 versus T-helper 17 involvement in ICI-pneumonitis—,putatively engaging in detrimental crosstalk with pro-inflammatory 'M1-like' monocytes. This finding yields several novel potential therapeutic targets for the treatment of ICI-pneumonitis. Most notably repurposing anti-IL-23 merits further research as a potential efficacious and safe treatment for ICI-pneumonitis.

WHAT IS ALREADY KNOWN ON THIS TOPIC

⇒ Immune checkpoint inhibitor (ICI)-pneumonitis is a frequent serious adverse event of cancer immunotherapy hinging on a cell-mediated immune response, though the exact pathophysiology is currently unknown.

WHAT THIS STUDY ADDS

⇒ Single-cell transcriptomics identifies enrichment of pathogenic (*TBX21, RORC, IFNG, IL-17A, CSF2* expressing) T-helper 17.1 cells and pro-inflammatory (*TNF*, *IL-1B*, *IL-6*, *IL-23A* expressing) monocytes in ICI-pneumonitis bronchoalveolar lavage fluid, putatively engaging in a feedforward inflammatory loop.

HOW THIS STUDY MIGHT AFFECT RESEARCH, PRACTICE OR POLICY

⇒ The data yield several novel potential therapeutic targets for ICI-pneumonitis. Notably anti-IL-23 holds promise as an efficacious and safe treatment for ICI-pneumonitis that deserves further research.

BACKGROUND

Immune checkpoint inhibitors (ICIs) have been approved for the treatment of many tumor types in various disease stages, offering

more durable responses and better tolerability compared with conventional cytotoxic treatments.[1] However, with the expanding use of ICIs, clinicians are increasingly confronted with immune-related adverse events (irAEs). While most of these side effects present with mild symptoms, some patients experience severe immune-mediated toxicity and require immunosuppressive therapy.[2] ICI-related pneumonitis (ICI-pneumonitis), most often occurring in patients with non-small cell lung cancer (NSCLC) treated with programmed cell death protein-1/programmed death ligand-1 (PD-1/PD-L1) blockade, is an irAE deserving special consideration. Its real-world incidence is up to 19%,[3] and it is the most frequent fatal adverse event in this patient population, responsible for 35% of iatrogenic deaths.[4] This reflects how difficult it remains to diagnose and effectively treat ICI-pneumonitis, as a result of the scarcity of available pathophysiological knowledge.[5 6]

Using flow cytometry, Suresh *et al* analyzed immune perturbations within the ICI-pneumonitis alveolar compartment, comparing bronchoalveolar lavage fluid (BALF) of 12 patients with ICI-pneumonitis to 6 ICI-treated patients without ICI-pneumonitis. They predominantly observed an increase of T cells in BALF. Particularly, CD4+ central memory T cells were increased, which on in vitro stimulation displayed increased tumor necrosis factor alpha (TNF-α) and interferon-gamma (IFN-γ) secretion, suggesting a T-helper 1 (T_{H1})-mediated immune response to underlie ICI-pneumonitis. Moreover, they observed that regulatory T cells (T_{REG}) had decreased immunoregulatory capacity, leading them to speculate that diminished immunosuppression by T_{REG} might trigger an exuberant T_{H1} immune response in ICI-induced pneumonitis. Myeloid cells also gained a more inflammatory phenotype in this study, expressing high levels of interleukin (IL)-1β and TNF-α.[7] In contrast, Wang *et al* profiled by flow cytometry longitudinally-collected peripheral blood mononuclear cells of 13 patients with ICI-pneumonitis and proposed a different mechanism. Particularly, they observed an increase in circulating T-helper 17 cells (T_{H17}), as well as an increase in the levels of IL-17 in plasma and BALF, suggesting an important role of T_{H17} in mediating ICI-pneumonitis.[8] A recent bulk transcriptomic study on surgical biopsies of eight ICI-pneumonitis lesions on the other hand, reported a predominant increase of CD8+ T cells and B cells.[9] Finally, two series of case reports in total encompassing five patients with ICI-pneumonitis reported a significant overlap between the T-cell receptor (TCR) repertoire of clonally-expanded BALF and tumor-infiltrating T cells, suggesting that antigens shared by the tumor and lung elicit the autoimmune response in ICI-pneumonitis.[10 11]

In summary, while the involvement of T cells in ICI-pneumonitis is clear, little is known about the contribution of specific T-cell subsets and the immune cells that modulate the T-cell response. This knowledge gap has direct clinical consequences, resulting in a lack of rational targeted therapies. To gain better insights into the mechanisms underlying ICI-pneumonitis, we performed deep immune profiling using single-cell RNA (scRNA-seq) and T-cell receptor sequencing (scTCR-seq) of ICI-pneumonitis BALF, and comparatively analyzed the bronchoalveolar immune landscape across patients with (lung) cancer with and without ICI-pneumonitis.

METHODS

We prospectively collected BALF from 11 patients (10 patients with NSCLC and 1 patient with melanoma) receiving anti-PD-1/PD-L1 treatment and developing ICI-pneumonitis. Diagnosis of ICI-pneumonitis was based on clinical, laboratory, radiographic and (invasive) microbiological findings. Grade was moderate to severe in all patients (grade 2–3 according to Common Terminology Criteria for Adverse Events (V.5.0), with only two patients requiring supplemental oxygen, and all patients received first-line treatment according to European Society for Medical Oncology guidelines.[2] Importantly, BALF was collected prior to the start of this treatment. We also analyzed BALF data from six control patients. These patients were demographically matched and underwent bronchoalveolar lavage of an unaffected (contralateral) lobe, solely for research purposes, during bronchoscopy with transbronchial biopsy of a newly diagnosed lung tumor. Detailed inclusion criteria as well as demographic and clinical data of the patient cohort are summarized in table 1, online Supplementary Table S1 and in the Supplementary Methods section.

Immediately after collecting BALF, cells were subjected to single-cell profiling using the 5' scRNA-seq kit from 10x Genomics. After quality control and filtering (online supplemental methods), we obtained ~775 million unique transcripts from 141,056 cells. Dimensionality reduction and clustering was performed using Seurat V.4.1.0.[12] Main cell types were annotated according to established marker gene panels (figure 1A,B). There was no evidence of clustering bias (ICI-pneumonitis vs control, or across individual patients; online supplemental figure S1).

To refine our subclustering efforts, we used additional samples profiled by scRNA-seq. Specifically, we pooled 3' scRNA-seq data of eight early-stage NSCLC tissue samples (~338 million unique transcripts from 72,170 cells) and seven normal lung samples (~134 million unique transcripts from 29,616 cells; online supplemental figure S2A).[13] Assignment of main cell types was done in a similar fashion as for the BALF data, without evidence of batch effects (NSCLC vs normal lung, or across individual patients; online supplemental figure S2B–D). Subsequently, data from each main cell type (derived from BALF, NSCLC and normal lung samples) were integrated separately using canonical correlation analysis, as described previously, without signs of batch effects across sequencing technologies, data sets or individual patients (online Supplemental figure S3).[14] After integration, subclustering of main cell types was done based on differential expression of marker genes.

Table 1 Demographics and characteristics of study cohort

	ICI-pneumonitis (n=11)	Control (n=6)	P value
Age, years	68.5 (61.7–72.8)	65.7 (53.0–75.9)	0.96
Sex	–	–	0.86
Men	5 (45.5)	3 (50.0)	
Women	6 (54.5)	3 (50.0)	
Smoking status	–	–	0.11
Never	1 (9.1)	3 (50)	
Former	9 (81.8)	2 (33.3)	
Active	1 (9.1)	1 (16.7)	
COPD	3 (27.3)	2 (33.3)	0.79
Underlying malignancy			
NSCLC	10 (90.9)	6 (100)	0.45
Melanoma	1 (9.1)	0 (0)	
Immunotherapy regimen			NA
Pembrolizumab	6 (54.5)	NA	
Nivolumab	1 (9.1)	NA	
Durvalumab	3 (27.3)	NA	
Atezolizumab	1 (9.1)	NA	
Prior systemic therapy*	8 (72.7)	NA	NA
Prior radiotherapy†	5 (45.5)	NA	NA
Time from symptom onset to sampling (days)	17.0 (9.0–19.0)	NA	NA
Grade‡			NA
2	9 (81.8)	NA	
3	2 (18.2)	NA	

Data are median (IQR) or n (%). The p values are from Mann-Whitney U test for continuous data and Pearson's $\chi 2$ for non-ordered categorical data, all based on a two-sided hypothesis.
*Last administration of chemotherapy at least 4 months prior to sampling.
†Radiotherapy completed at least 3 months prior to sampling.
‡Grading according to Common Terminology Criteria for Adverse Events V.5.0.
COPD, chronic obstructive pulmonary disease; ICI, immune checkpoint inhibitor ; NSCLC, non-small cell lung cancer.

To gain information on clonotype distribution and dynamics, we performed scTCR-seq on these samples and considered all productive TCRs, which we defined as T cells with TCRs that can be joined in a reading frame by V(D)J recombination without premature stop codons, enabling assessment of a complete TCR α or β chain for downstream analysis. Relative clonotype richness was defined as the number of unique TCRs divided by the total number of cells with a unique TCR. Clonotype evenness was assessed by calculating the inverse Simpson index divided by the number of unique clonotypes. Gini coefficient, a summary metric of inequality of clonotype distribution within a repertoire, was calculated using the 'Gini' function from the DescTools R package.[15 16]

We used the CellRank algorithm to functionally characterize CD4+ T-cell state transitions, based on transcriptional similarity between cells and RNA velocity.[17]

A detailed workflow of downstream analyses is provided in the online supplemental methods section.

RESULTS

T cells dominate the bronchoalveolar space in ICI-pneumonitis

After quality control and filtering (online supplemental methods), we obtained 141,056 cells of which 85,481 were derived from ICI-pneumonitis BALF and 55,575 from demographically-matched control BALF. We identified several clusters, which we linked to cell types (figure 1A) based on canonical marker gene expression (figure 1B), and we then evaluated differences in immune cell proportions (figure 1C). T cells made up more than half of all immune cells in ICI-pneumonitis BALF, a striking fourfold increase compared with control BALF. Conversely, we observed a clear relative depletion of monocytes/macrophages in ICI-pneumonitis BALF, while dendritic cells (DCs) were threefold increased. For B cell, neutrophil and mast cell abundance, no statistically significant differences between ICI-pneumonitis and control BALF were observed.

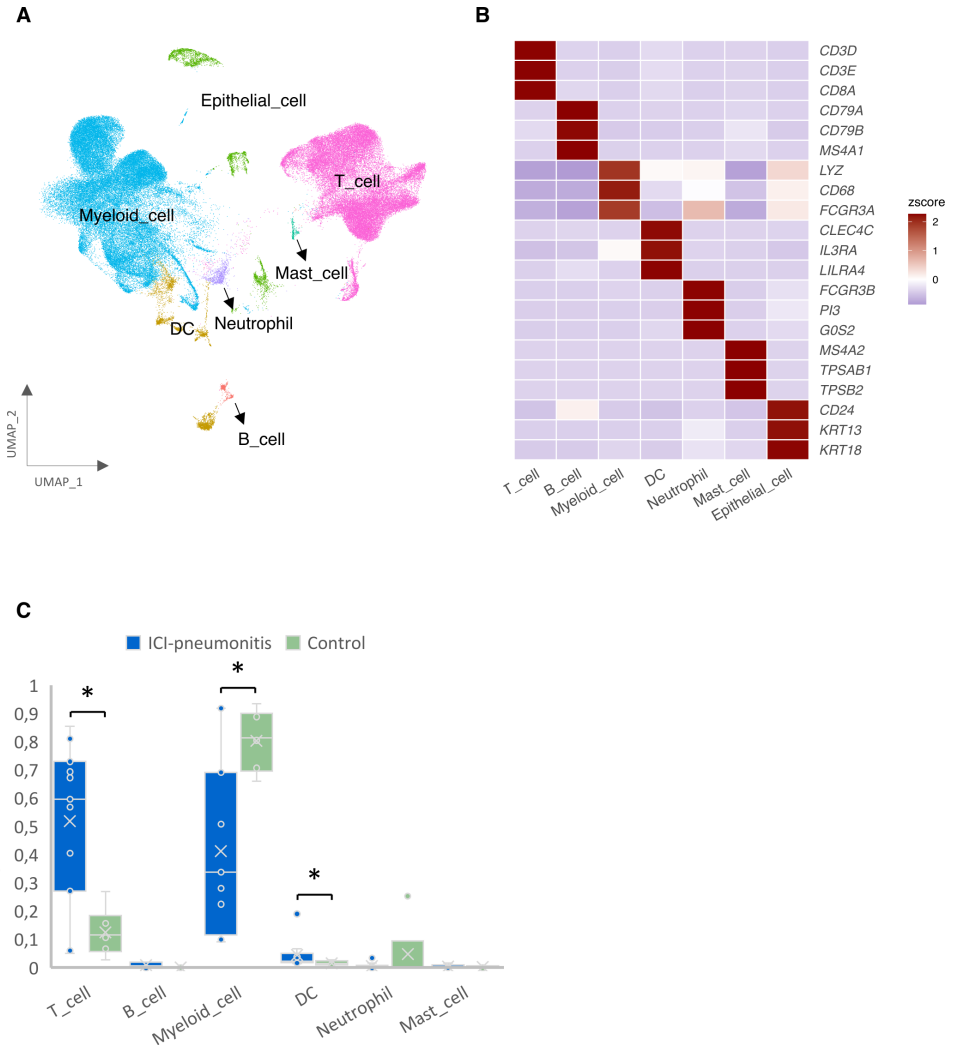

Figure 1 Cell composition of ICI-pneumonitis and control patients' bronchoalveolar lavage fluid (BALF). (A) UMAP plot of 141,056 cells present in ICI-pneumonitis and control BALF. (B) Heatmap of canonical marker gene expression used for main cell type annotation. (C) Comparison of relative cell type abundance, revealed accumulation of T cells and dendritic cells in ICI-pneumonitis BALF, while other myeloid cells (monocytes/macrophages) were relatively depleted. Wilcoxon rank-sum test was used; significance is shown as *p<0.05. DC, dendritic cell; ICI, immune checkpoint inhibitor; UMAP, Uniform Manifold Approximation and Projection.

Altogether, these broad immune cell typing efforts confirm previous reports highlighting prominent T-cell involvement in ICI-pneumonitis, but they fail to point towards neutrophil or B cell involvement.[7 9] Furthermore, we describe enrichment of DCs as a novel characteristic of BALF from ICI-induced pneumonitis.

Pathogenic CD4+ $T_{H17.1}$ and effector memory CD8+ T cells in ICI-pneumonitis BALF

To better characterize the T-cell response, we subclustered all 65,293 T cells and performed an in-depth analysis of T-cell subclusters. Overall, we identified seven CD4+ T-cell subtypes; naïve-like (T_N; with *CCR7, LEF1* and *TCF7* as marker genes), effector memory ($T_{EM;}$ *ANXA1, CXCR4, IL-2*), T follicular helper (T_{FH}; *BCL6, CXCR5, ICA1*), two clusters of T_{REG} and two clusters of CD4+ T cells with both (T_{H17}-like; *RORC, IL-23R, CCR6*) and (T_{H1}-like; *TBX21, IFNG, CXCR3*) properties, termed $T_{H17.1}$ cells (figure 2A,B; online supplemental figure S4A). T_{REG} consisted of a *FOXP3*+ T_{REG} cluster (T_{REG}; *FOXP3, IL-2RA, IL-1R2*) and *FOXP3*– regulatory type 1 T-cell cluster (T_{R1}; *CRTAM, IL-10, LAG3*), which derive from T-helper, CD4+ naïve or memory T cells in inflamed peripheral organs where they induce tolerance, mainly by producing IL-10 and by selective killing of antigen-presenting cells (APCs) through granzyme B and perforin secretion.[18] Indeed, the cytotoxic capacity of these CD4+ T cells explains why they cluster in close proximity to CD8+ T cells on the Uniform Manifold Approximation and Projection plot (online supplemental figure S4B). $T_{H17.1}$ cells finally constituted a large cluster, termed $T_{H17.1\_RORC}$ cells, with balanced expression of T_{H1}-related and T_{H17}-related genes, and a smaller cluster, termed $T_{H17.1\_TBX21}$ cells, with a pronounced pathogenic phenotype evidenced by retained T_{H17}-related gene expression (*RORC, CCR6, IL-17A, IL-23R*), but

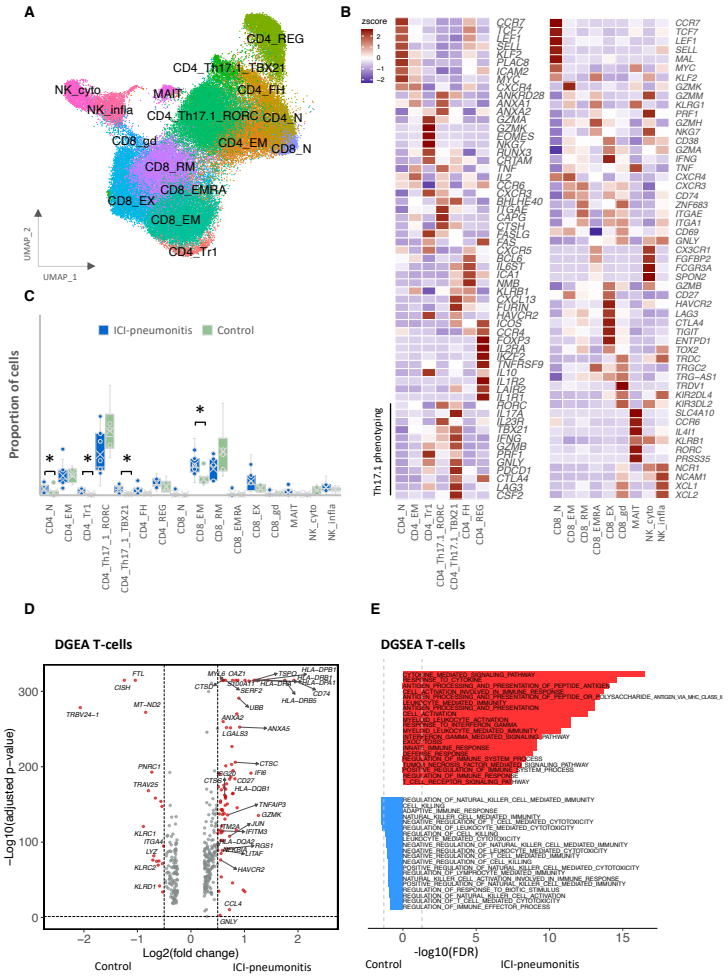

Figure 2 T-cell phenotypes and relative abundance in ICI-pneumonitis and control bronchoalveolar lavage fluid. (A) Uniform Manifold Approximation and Projection plot of 65,293 T cells, (B) annotated according to canonical marker gene expression of CD4+ (left panel) and CD8+ T cells, MAIT, and NK-cells (right panel). (C) A comparison of relative T-cell subtype abundance, revealed accumulation of CD4+ T-helper 17.1 cells with a pathogenic phenotype ($T_{H17.1\_TBX21}$) in ICI-pneumonitis, as well as enrichment of CD4+ regulatory type 1 T cells (T_{R1}), $CD4^+$ naïve-like T cells (T_N), and CD8+ effector memory (T_{EM}) T cells. Wilcoxon rank-sum test was used; significance is shown as *p<0.05. (D) Volcano plot showing differentially expressed genes in T cells comparing ICI-pneumonitis and control T cells. P values were obtained by the model-based analysis of single-cell transcriptomics (MAST) test and Bonferroni-corrected (see online supplemental table S1 for all differentially expressed genes). (E) Differential gene set enrichment analysis (DGSEA) on differentially expressed genes for ICI-pneumonitis versus control T cells using the R package hypeR. Only significant genes (adjusted p value<0.05) and genes with a log-fold change higher than 0.5 or lower than −0.5 were used (see online supplemental tables S2 and S3 for all differentially expressed gene sets in ICI-pneumonitis and control T cells, respectively). CD4_N, CD4+ naïve-like T cells; CD4_EM, CD4+ effector memory T cells; CD4_TR1, CD4+ regulatory type 1 T cells; CD4_Th17.1_RORC, CD4+ T-helper 17.1 lymphocytes with predominant non-pathogenic features; CD4_Th17.1_TBX21, CD4+ T-helper 17.1 lymphocytes with predominant (pathogenic) T-helper 1-like features; CD4_FH, CD4+ follicular helper T-cells; CD4_REG, CD4+ regulatory T cells; CD8_N, CD8+ naïve-like T cells; CD8_EM, CD8+ effector memory T cells; CD8_RM, CD8+ resident memory T cells; CD8_EMRA, CD8+ recently activated effector memory T cells; CD8_EX, CD8+ exhausted T cells; CD8_gd, CD8+ gamma delta T cells; DGEA, differential gene expression analysis; FDR, false discovery rate; ICI, immune checkpoint inhibitor; MAIT, mucosal associated invariant T cells; NK, natural killer; NK_cyto, cytotoxic NK-cells; NK_infla, inflammatory NK-cells.

upregulation of T_{H1}-related (*TBX21, IFNG),* cytotoxicity-related (*GZMB, PRF1, GNLY*), exhaustion-related (*PDCD1, CTLA4, LAG3*) and monocyte activation-related genes (*CSF2,* encoding granulocyte-macrophage colony-stimulating factor (GM-CSF)).[19]

Next, we identified seven CD8+ T-cell subtypes, namely (T_N; *CCR7, LEF1, TCF7*), (T_{EM}; *GZMK, GZMM, CXCR4*), resident-memory (*ZNF683, ITGAE, ITGA1*), recently activated effector memory (*CX3CR1, FGFBP2, FCGR3A*) and experienced (co-expressing effector markers *GZMB,*

PRF1, GNLY, IFNG and inhibitory checkpoint molecules *HAVCR2, CTLA4, LAG3*) CD8+ T cells, as well as the innate-like lymphoid gamma delta T cells ($T_{\gamma\delta}$; *TRDC, KIR3LD2, KIR3LD4*) and mucosal associated invariant T cells (T_{MAIT}; *RORC, IL-23R, SLC4A10*). Finally, we found two natural killer (NK) cell populations, namely inflammatory and cytotoxic NK-cells marked by immune cell recruitment (*NCAM1, NCR1, XCL1, XL2*) and cytotoxic functions (*PRF1, FCGR3A, CX3CR1, FGFBP2*), respectively.

When comparing the relative proportions of T-cell subtypes in ICI-pneumonitis and control BALF, CD4+ $T_{H17.1}$ cells were most frequent, accounting for one-third of all T cells in both conditions. Particularly, CD4+ $T_{H17.1}$ cells corresponded to 13% of all immune cells in ICI-pneumonitis versus 3% in control BALF. Within CD4+ $T_{H17.1}$ cells, we noticed no significant differences between ICI-pneumonitis and control BALF for $T_{H17.1\_RORC}$ cells, but a fourfold increase in pathogenic (*IFNG*^{high}, *CSF2*^{high}) $T_{H17.1\_TBX21}$ cells (figure 2C). $T_{H17.1}$ cells are increasingly recognized for their role in autoimmune processes, for example, sarcoidosis and inflammatory bowel disease (IBD), in which their capacity for IFN-γ secretion correlates to disease severity.[20 21] More recently, it has become clear that also GM-CSF secretion by these T-helper cells is a critical regulator of auto-inflammation, for example, in multiple sclerosis where IFN-γ+ GM-CSF+ T-helper cells license myeloid cells for tissue destruction.[19]

CD4+ T_N cells were also more abundant in ICI-pneumonitis BALF, as were (*IL-10*^{high}) CD4+ T_{R1} cells. The latter have been shown to arise during $T_{H17.1}$-mediated inflammation as a negative feedback mechanism, and the abundance of T_{R1} cells indeed was higher in patients with ICI-pneumonitis showing resolution of radiographic abnormalities after first-line treatment compared with patients with persistent abnormalities (online supplemental figure S4C).[22] Finally, a slight increase in CD4+ T_{FH} abundance, although not significant (p=0.18), was observed in ICI-pneumonitis BALF, which correlates with previous observations in a patient with inherited PD-1 deficiency, developing severe autoimmune pneumopathy.[23] No statistically significant differences were observed regarding the relative abundance of other CD4+ T-cell subtypes. In the CD8+ T-cell compartment, we found enrichment of CD8+ T_{EM} in ICI-pneumonitis compared with control BALF; a T-cell subset with an activated phenotype (high expression of *CD27* and *CD69*; low expression of inhibitory checkpoints *HAVCR2, TIGIT, CTLA4*) that contributes to an inflammatory tissue response (*GZMK, GZMA, TNF*).[24] No significant differences were seen for other conventional CD8+ T-cell subtypes, nor for $T_{\gamma\delta}$, T_{MAIT} or NK-cells.

Interestingly, an unbiased differential gene expression analysis (DGEA) coupled to differential gene set enrichment analysis (DGSEA) on all T cells (figure 2D,E), confirmed the presence of a highly activated T-cell compartment in ICI-pneumonitis BALF (upregulation of co-stimulatory receptor *CD27;* MHC class II genes *HLA-DRB1, HLA-DRB5, HLA-DPB1; ITM2A*) with pro-inflammatory and cytotoxic features (NF-κB (*NFKBIA, TNFAIP3*) and AP-1 (*JUN*) signaling*; CCL4; GZMK; GNLY*), and marked upregulation of genes related to interferon signaling (*IFI6, ISG20, IFITM3, RGS1*).

Overall, these scRNA-seq analyses showed massive T-cell accumulation in ICI-pneumonitis BALF, of which $T_{H17.1}$ cells made up the largest fraction. Comparing relative T-cell subtype abundance within the T-cell compartment, identified preferential enrichment of *IFNG*^{high}, *CSF2*^{high} $T_{H17.1\_TBX21}$ cells in ICI-pneumonitis. This finding provides an explanation for previous contradictory T-cell phenotyping efforts in ICI-pneumonitis, in which presumably these hybrid $T_{H17.1}$ cells were named either T_{H1} or T_{H17} cells.[7 8] In line with prior studies, we observed accumulation of CD8+ T_{EM}, likely contributing to the excessive type 1 immune response, and CD4+ T_N, that via CD62L (*SELL*) could possibly be recruited to the site of inflammation.[7] Finally, we observed a slight enrichment of *IL-10*^{high} T_{R1} cells, a regulatory cell type relying mainly on IL-10 secretion and APC killing to exert its function, suggesting they represent a negative feedback mechanism counterbalancing $T_{H17.1}$-mediated inflammation. Indeed, although enrichment of an IL-10 secreting regulatory cell type may seem counterintuitive, increased systemic levels of IL-10 during ICI-pneumonitis development have been reported previously.[25 26]

Cell fate mapping and TCR analysis reveals pathogenic phenotype shift of T-helper cells

The above analyses suggested a central role for a pathogenic subset of $T_{H17.1}$ cells in ICI-pneumonitis pathophysiology. To more comprehensively characterize the $T_{H17.1}$ immune response, we performed single-cell fate mapping and continuous gene expression analysis by running the CellRank algorithm on CD4+ T cells.[17] This algorithm ranks individual cells based on similarity in gene expression and RNA velocity along probabilistic state-change trajectories. It allows to study and compare relatedness and gene expression dynamics of cell subtypes between different conditions in a continuous manner. After we excluded T_{REG} from these analyses given their distinct developmental paths,[27] we identified a trajectory in which T_{EM} were connected to the $T_{H17.1\_RORC}$ cluster, which then branched into either $T_{H17.1\_TBX21}$ or T_{R1} as terminal states, or formed a terminal state itself (figure 3A,B). We confirmed this trajectory by independent TCR repertoire analysis, showing the highest degree of TCR sharing between connected cell states (online supplemental figure S4D,E).

We next plotted key marker and functional genes, as well as the relative abundance of cells in ICI-pneumonitis and control samples, along the $T_{H17.1\_TBX21}$ trajectory (figure 3C,D). This analysis showed progressive downregulation of naïve state genes (*TCF7, IL-7R*, lymph node homing receptor *CCR7*) and upregulation of T_{H17}-related genes (*RORC, CCR6, IL-23R*) early in the trajectory. At this stage, where cell density is still high for control samples, we observed co-expression of non-pathogenic

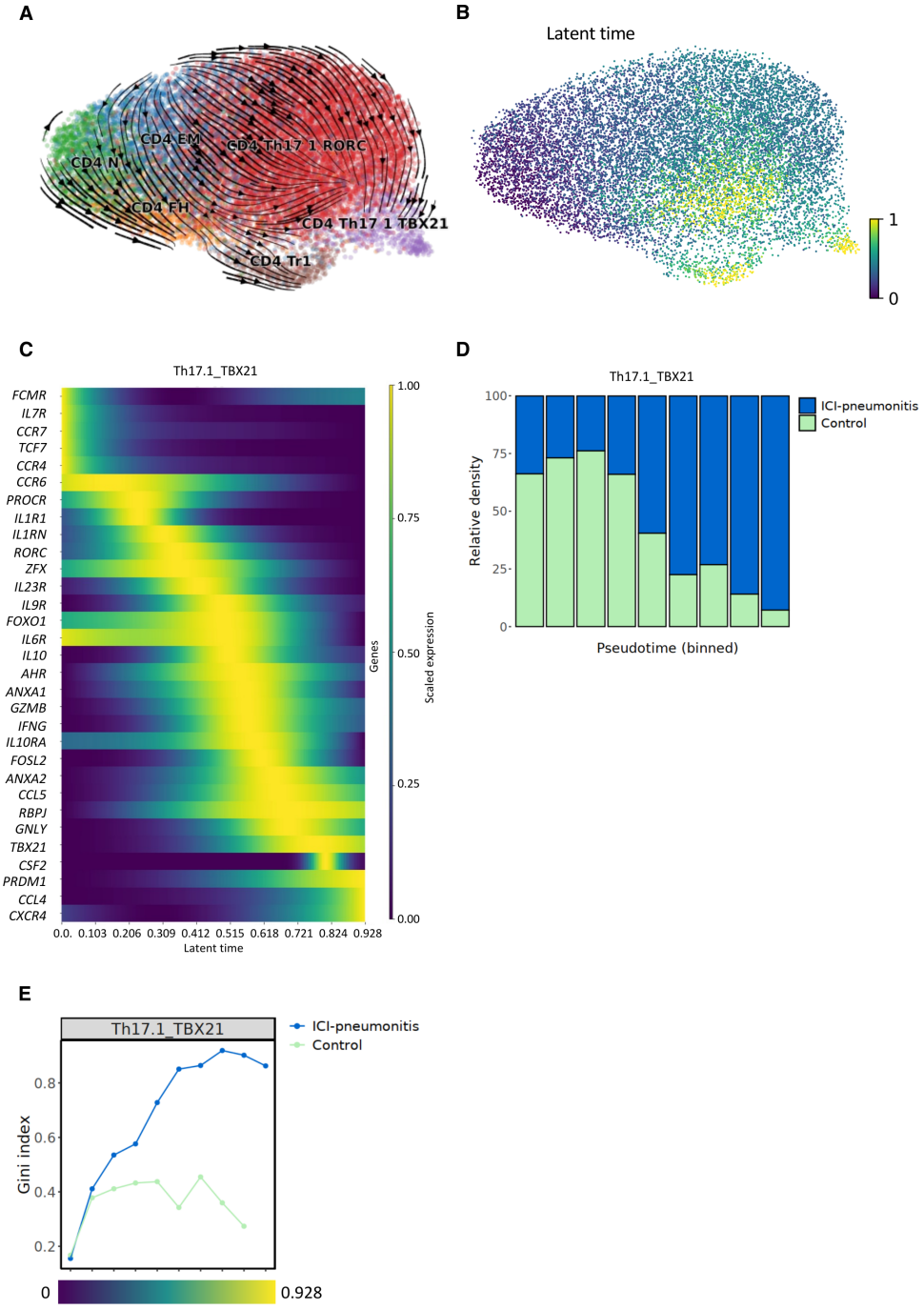

Figure 3 Cell fate mapping and T-cell receptor repertoire analysis of CD4+ T cells in ICI-pneumonitis and control bronchoalveolar lavage fluid. (A) Uniform Manifold Approximation and Projection plot of 11,570 CD4+ T cells with cell fate trajectories and (B) latent time as calculated by the CellRank algorithm, showing T_{EM} were connected to the $T_{H17.1\_RORC}$ cluster, which branched into either $T_{H17.1\_TBX21}$ or T_{R1} as terminal states, or formed a terminal state itself. (C) Continuous gene expression profiling along the $T_{H17.1\_TBX21}$ trajectory. (D) Barplot of relative cell abundance in ICI-pneumonitis and control bronchoalveolar lavage fluid (BALF) along the $T_{H17.1\_TBX21}$ trajectory. (E) Line graph of the Gini coefficient for ICI-pneumonitis and control BALF T-cell receptor repertoire along the $T_{H17.1\_TBX21}$ trajectory, as calculated by the DescTools algorithm. CD4_N, CD4+ naïve-like T cells; CD4_EM, CD4+ effector memory T cells; CD4_TR1, CD4+ regulatory type 1 T cells; CD4_Th17.1_RORC, CD4+ T-helper 17.1 lymphocytes with predominant non-pathogenic features; CD4_Th17.1_TBX21, CD4+ T-helper 17.1 lymphocytes with predominant (pathogenic) T-helper 1-like features; CD4_FH, CD4+ follicular helper T cells; ICI, immune checkpoint inhibitor.

transcription factors, for example, *ZFX* (driving a T_{H17} self-renewal program) and *FOXO1* (downregulating inflammatory cytokine secretion), coupled to expression of mostly non-pathogenic surface molecules and cytokines; *PROCR* (which negatively regulates pro-inflammatory cytokine secretion), *IL-1RN* (encoding IL-1 receptor antagonist, unexpectedly co-expressed with IL-1 receptor *IL-1R1*), *IL-6R* (which 'stabilizes' non-pathogenic T_{H17}-like

cells), *IL-10*, and *IL-10RA* (encoding IL-10 receptor).[28–31] Further along the trajectory, transcription factors associated with a pathogenic phenotype are upregulated, most notably *TBX21* (inducing a.o. IFN-γ secretion) and *PRDM1* (encoding BLIMP-1, a transcription factor promoting a.o. GM-CSF secretion). As a result, pro-inflammatory chemokines (*CCL4, CCL5*), cytotoxicity genes (*GZMB, GNLY*), and especially key genes mediating $T_{H17.1}$ pathogenicity, namely *IFNG* and *CSF2*, are progressively upregulated near the end of the $T_{H17.1}$ trajectory, where cell density peaks for ICI-pneumonitis BALF samples.[32 33]

In a similar fashion, we comparatively examined T-cell clonality along the $T_{H17.1\_TBX21}$ trajectory, obtaining 11,570 CD4+ T cells with a TCR sequence. To assess clonotype diversity and distribution, we calculated TCR richness and evenness as well as the Gini coefficient (figure 3E; online supplemental figure S4F). While low TCR richness indicates a limited number of T-cell specificities, low evenness marks a skewed distribution of these specificities. The Gini coefficient is a summary metric of inequality of clonotype distribution within a repertoire, such that a high Gini coefficient and low TCR richness and evenness reflect clonal expansion of specific T-cell clones following cognate antigen recognition.[15] We observed a progressive increase of the Gini coefficient, and a decline of TCR richness and evenness, along the $T_{H17.1\_TBX21}$ trajectory in ICI-pneumonitis, which was not seen in control BALF. This suggests strong antigen-driven clonal proliferation of $T_{H17.1\_TBX21}$ cells, another established feature of pathogenic $T_{H17.1}$ cells.[33]

Overall, cell fate mapping coupled to single-cell TCR repertoire analysis unraveled the plasticity of $T_{H17.1}$ cells in ICI-pneumonitis and control BALF. These cells are skewed towards a pathogenic *IFNG*^{high} *CSF2*^{high} phenotype in ICI-pneumonitis BALF, regulated by transcription factors *TBX21* and *PRDM1*, respectively. Importantly, T-cell clonality analyses showed pronounced antigen-driven clonal expansion of this phenotype, further supporting the notion that these are not just bystander activated T cells but central players in ICI-pneumonitis pathophysiology.[33]

Crosstalk between pathogenic $T_{H17.1}$ cells and pro-inflammatory monocytes

We next wondered how innate immune cells are involved in ICI-pneumonitis immunopathology, and subclustered all 63,330 monocytes and macrophages (figure 4A–C). First, monocytes were separated from macrophages based on differential canonical monocyte (*FCN1, LILRB2, LILRA5*) or macrophage marker gene expression (*PPARG, FABP4, MARCO*), respectively. Monocytes were then subclustered into classical FCN1^{high} (*FNC1, S100A8, S100A9*) and inflammatory IL-1B^{high} monocytes (*IL-1B, CCL20, IL-6*). Within the macrophages, we identified monocyte-derived (expressing *LGMN, CHI3L1* and *MERTK*) and tissue-resident FABP4^{high} alveolar macrophages (*FABP4, PPARG, MARCO*), which formed a non-proliferating and a proliferating subcluster (*MKI67, TOP2A, CDK1*). We observed a significant decrease of anti-inflammatory alveolar macrophages in ICI-pneumonitis BALF, and a corresponding increase of monocyte-derived macrophages and pro-inflammatory *IL-1B*^{high} monocytes (figure 4D).

Besides *IL1B*, these pro-inflammatory monocytes show high expression of other pro-inflammatory genes, most notably *TNF* (encoding TNF-α), *IL-6, IL-23A, CSF2RA, CSF2RB, CCL20* and the interferon-induced chemokines *CXCL9/10*. CXCL9/10 and CCL20 are potent chemoattractants of CXCR3+ and CCR6+ cells, respectively, with presence of both chemotaxis receptors defining $T_{H17.1}$ cells.[34] IL-1 and IL-23 moreover are critical cytokines inducing pathogenic features (notably GM-CSF secretion) in $T_{H17.1}$ cells.[19] Reciprocally, GM-CSF signaling through the GM-CSF receptor (*CSF2RA*, *CSF2RB*) is known to induce this pro-inflammatory monocyte phenotype.[19] DGEA and DGSEA across all monocytes/macrophages comparing ICI-pneumonitis and control BALF, confirmed that pro-inflammatory *IL-1B*^{high} monocytes are involved in the innate immune response in ICI-pneumonitis (figure 4E,F). Specifically, expression of pro-inflammatory 'M1-like' genes (*CCL3, CCL4, IL1B, TNF, NFKBIA*) was upregulated in ICI-pneumonitis monocytes/macrophages, while anti-inflammatory 'M2-like' genes (*IGF1, MARCO*) were relatively enriched in control monocytes/macrophages.

We also analyzed the DC compartment in a similar fashion, as these cells have a central role in directing T-cell phenotypes. Subclustering of DCs revealed classical type I DCs (*CLEC9A, XCR1, CPNE*), type II DCs (*CLEC10A, FCGR2B, FCER1G*), plasmacytoid DCs (*LILRA4, CLEC4C, IRF7*), and migratory DCs (*CCR7, LAMP3, FSCN1*) (figure 5A,B). Although DCs were overall enriched in ICI-pneumonitis BALF, we observed no significant differences for DC subtype abundance between ICI-pneumonitis and control BALF (figure 5C). Hence, the role of DCs in shaping the ICI-pneumonitis immune response remains unclear. Our data do suggest, however, that myeloid cells, specifically pro-inflammatory monocytes, might not only directly mediate tissue damage in ICI-pneumonitis but also sustain tissue inflammation by recruiting and shaping pathogenic $T_{H17.1}$ cells under the influence of GM-CSF.[19]

DISCUSSION

Here, we shed light on the mechanisms underlying pneumonitis occurring in patients with cancer during anti-PD-1/PD-L1 therapy. These findings are important, as they are a necessary first step to identifying immunomodulatory treatments effectively targeting the root cause of ICI-pneumonitis. These are currently lacking, making ICI-pneumonitis the most frequent fatal anti-PD-1/PD-L1-related adverse event.[4] For the first time, we present a single-cell transcriptomic atlas of the bronchoalveolar immune landscape in ICI-pneumonitis, comparing the relative abundance of immune cell types as well as their precise phenotype and clonotype distribution to those in BALF of demographically-matched controls.

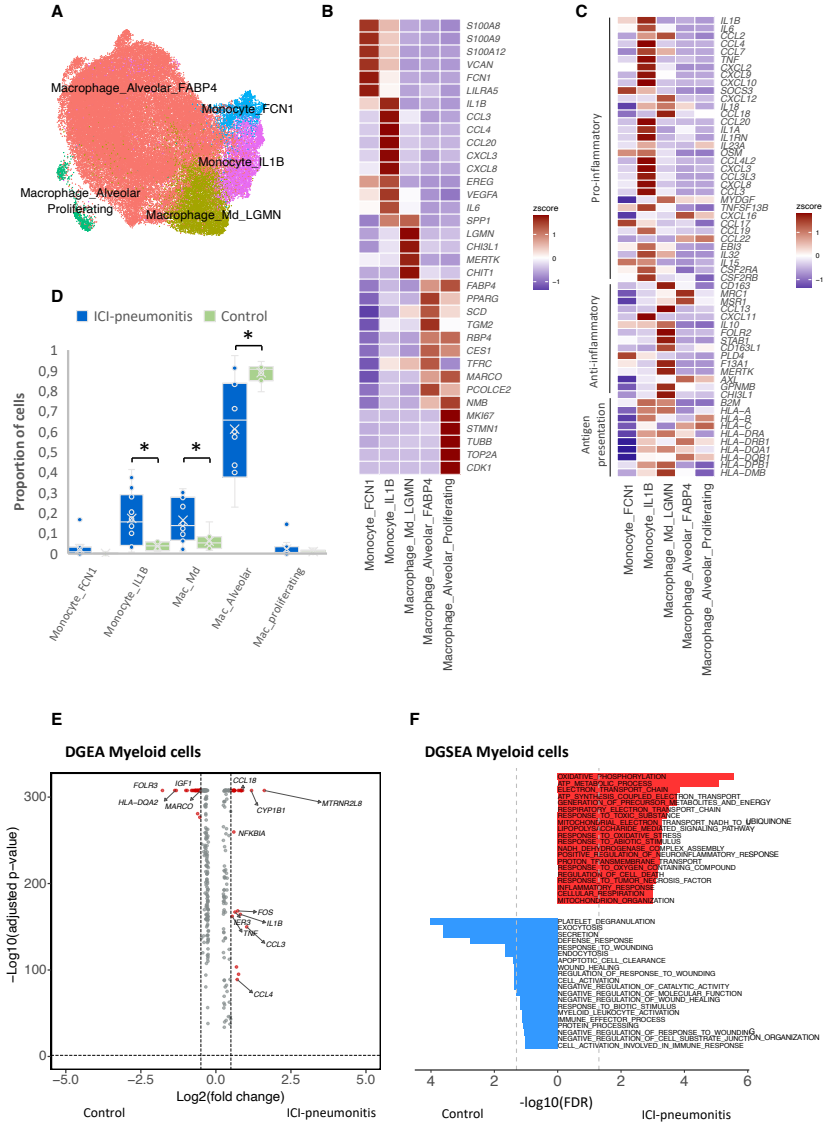

Figure 4 Macrophage and monocyte phenotypes and relative abundance in ICI-pneumonitis and control bronchoalveolar lavage fluid. (A) Uniform Manifold Approximation and Projection plot of 63,330 macrophages and monocytes, (B) annotated according to canonical marker gene expression. (C) Heatmap of functional gene expression patterns in macrophages and monocytes, showing pro-inflammatory/anti-inflammatory and antigen presentation-related gene expression patterns. (D) Comparison of relative cell subtype abundance, showing a relative enrichment of monocyte-derived macrophages (Mac_Md) and *IL-1B*^{high} pro-inflammatory monocytes (Monocyte_IL-1B) and a relative depletion of alveolar resident macrophages (Mac_Alveolar) in ICI-pneumonitis bronchoalveolar lavage fluid. Wilcoxon rank-sum test was used; significance is shown as *p<0.05. (E) Volcano plot showing differentially expressed genes in monocytes/macrophages comparing ICI-pneumonitis and control samples. P values were obtained by the model-based analysis of single-cell transcriptomics (MAST) test and Bonferroni-corrected (see online supplemental table S4 for all differentially expressed genes). (F) Differential gene set enrichment analysis (DGSEA) on differentially expressed genes for ICI-pneumonitis versus control monocytes/macrophages using the R package hypeR. Only significant genes (adjusted p value<0.05) and genes with a log-fold change higher than 0.5 or lower than −0.5 were used (see online supplemental table S5 and S6 for all differentially expressed gene sets in ICI-pneumonitis and control monocytes/macrophages, respectively). DGEA, differential gene expression analysis; FDR, false discovery rate; ICI, immune checkpoint inhibitor; IL, interleukin; Macrophage_Md_LGMN monocyte-derived macrophage.

First and foremost, we confirm that T-cell accumulation, of both CD4+ and CD8+ T cells, is a hallmark of ICI-pneumonitis. T cells constitute about 10% of immune cells in control BALF (in line with historical findings in healthy BALF),[35] whereas they make up more than half of all immune cells in ICI-pneumonitis BALF. $T_{H17.1}$ cells, which are T_{H17} cells that have gained T_{H1} features such as expression of transcription factor T-bet (encoded by *TBX21*) and IFN-γ (*IFNG*), make up the bulk of T cells in both ICI-pneumonitis and control BALF (which

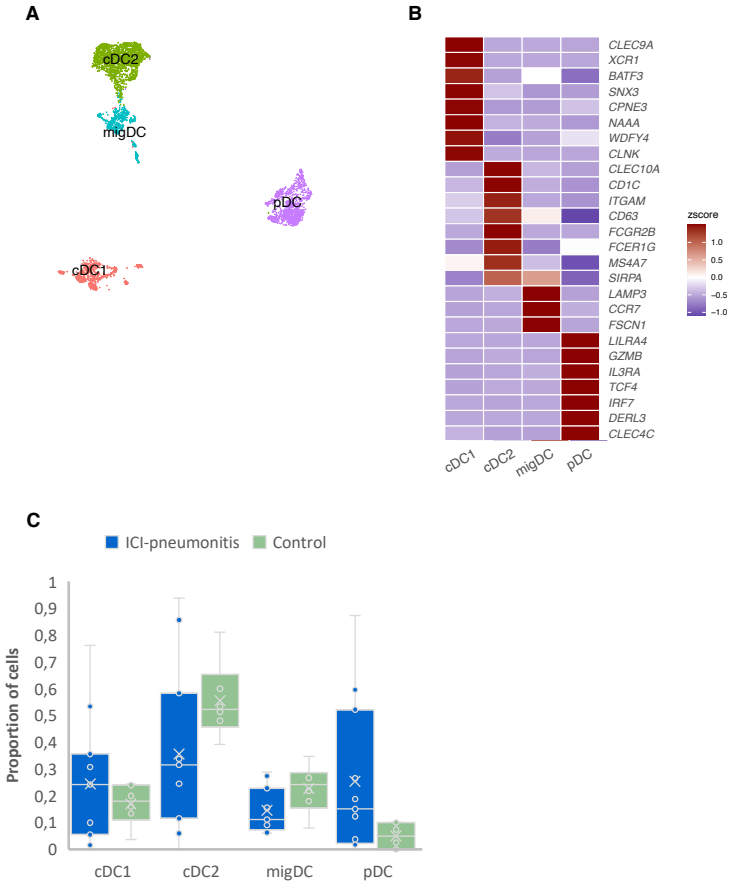

Figure 5 Dendritic cell phenotypes and relative abundance in ICI-pneumonitis and control bronchoalveolar lavage fluid. (A) Uniform Manifold Approximation and Projection plot of 2642 dendritic cells, (B) annotated according to canonical marker gene expression. (C) A comparison of relative dendritic cell subtype abundance showed no statistically significant differences between ICI-pneumonitis and control bronchoalveolar lavage fluid. Wilcoxon rank-sum test was used. cDC1, classical type I dendritic cell; cDC2, classical type II dendritic cell; ICI, immune checkpoint inhibitor; migDC, migratory dendritic cell; pDC, plasmacytoid dendritic cell.

corresponds to a fourfold increase of the ratio of $T_{H17.1}$ cells over all immune cells in ICI-pneumonitis). More importantly we show, both by subclustering and by fate mapping of $T_{H17.1}$ cells coupled to TCR repertoire analysis, that they display a more pathogenic phenotype evidenced by higher expression of *IFNG*, *CSF2* (encoding GM-CSF) and cytotoxicity genes and by strong antigen-driven clonal proliferation. This cell type is increasingly being recognized in autoimmune processes, such as IBD, multiple sclerosis and sarcoidosis, previously thought to have been mediated by T_{H1} cells.[33] The type 1 immune response conveyed by $T_{H17.1}$ cells is probably strengthened by CD8+ effector memory T cells, which were more abundant in ICI-pneumonitis BALF. Earlier studies on

ICI-pneumonitis also observed prominent lymphocytosis, with higher abundance of TNF-α^{high} CD8+ T cells,[7] but contradictory findings were reported on T_{H1} versus T_{H17} involvement. We argue this might be due to limited flow cytometry panels used in these studies (compared with whole-transcriptome scRNA-seq data) that did not include the canonical T_{H17} transcription factor antibody anti-RORγ, hence precluding the identification of a hybrid $T_{H17.1}$ phenotype.[7 8]

Second and somewhat unexpectedly, we observed a higher abundance of *FOXP3*$^{-}$ *IL-10*^{high} T_{R1} in ICI-pneumonitis BALF. In preclinical models, it has been shown that in pro-inflammatory conditions, in the presence of TGF-β/IL-6/IL-23, T_{H17} cells are skewed towards a pathogenic $T_{H17.1}$ phenotype but that a small proportion of these $T_{H17.1}$ cells gives rise to T_{R1} cells, in line with our findings.[22] Indeed, while IL-10 is the prototypical anti-inflammatory IL, increased serum IL-10 levels have been reported during ICI-pneumonitis.[25 26]

How innate immune cells interact with $T_{H17.1}$ cells in ICI-pneumonitis remains speculative, but our scRNA-seq data provide a solid basis for hypothesis generation. First, we show that anti-inflammatory phagocytosing alveolar resident macrophages are depleted, while monocyte-derived macrophages and pro-inflammatory *IL-1B*^{high} monocytes are relatively enriched in ICI-pneumonitis BALF. A detrimental feedforward loop in which pathogenic T-helper cell-derived GM-CSF instructs GM-CSF receptor expressing monocytes to orchestrate tissue inflammation (TNF-α, IL-6) and tissue damage (reactive oxygen species) while sustaining pathogenic T-helper cells (through IL-23 secretion, intensified by IL-1β secretion), is a well-established mechanism of auto-inflammation, best characterized in multiple sclerosis but also discerned in one patient with inherited PD-1 deficiency.[19 23 36] In line with this mechanism, is a prior study in which elevated levels of GM-CSF at baseline and early during ICI treatment were found to predict severe irAEs.[37] In addition, the pro-inflammatory monocytes might recruit *CXCR3*- and *CCR6*-expressing $T_{H17.1}$ cells through expression of the chemoattractants *CXCL9/CXCL10* and *CCL20*, respectively.[38 39] Notably, an increase of serum CXCL9/10 concentrations after anti-PD-1/PD-L1 therapy, was shown to predict occurrence of irAEs.[40]

Lastly, we expected a role for DCs in instructing pathogenic $T_{H17.1}$ cells, based on their known role as orchestrators of adaptive immunity and their increased abundance in ICI-pneumonitis BALF. However, subclustering analysis did not reveal a clear phenotypic shift of DCs. As such, our data do not provide insights into the role of DCs in ICI-pneumonitis pathophysiology. Possibly, profiling of regional lymph nodes is necessary to reveal relevant DC/T-cell interactions, as was the case for IL-23-producing DCs residing in mesenteric lymph nodes of patients with IBD.[41]

Our findings bear important potential to improve the care of patients with anti-PD-1/PD-L1 treated cancer experiencing ICI-pneumonitis. Although 70–80% of symptomatic ICI-pneumonitis cases resolve with corticosteroid treatment,[42] it cannot be formally excluded that corticosteroids negatively impact tumor control.[43] Moreover, second-line treatment for steroid-refractory ICI-pneumonitis lacks a clear scientific rationale and success rates are therefore modest.[42] Our findings advocate clinical trials with agents targeting crosstalk between pathogenic $T_{H17.1}$ cells and pro-inflammatory monocytes. Although GM-CSF emerges as the master regulator, it has important homeostatic functions in the lungs and its role in antitumor immunity is ambiguous.[44] Anti-IL-6 and anti-TNF-α therapy tackles monocyte-mediated tissue inflammation, and has indeed shown efficacy and safety as second-line treatment for steroid-refractory irAEs in limited case series,[45] but does not disrupt the interplay between pathogenic $T_{H17.1}$ cells and pro-inflammatory monocytes. Based on our data, we speculate that repurposing anti-IL-1 and especially anti-IL-23 risankizumab might improve response rates without negatively affecting tumor control.[45]

A potential limitation of the study is that all recruited patients with ICI-pneumonitis had limited grade pneumonitis and did not require second-line immunosuppressive therapy. As such, we cannot exclude that distinct disease processes take place in high grade or steroid-refractory ICI-pneumonitis. Second, while the control cohort of patients was demographically matched to the study cohort (also with regards to smoking status, lung disease and the presence of a thoracic malignancy, importantly), these patients did not receive prior anti-PD-1/PD-L1 treatment. All BALF samples were taken during routine bronchoscopy so we could minimize patients' exposure to the risks of this invasive procedure, knowing that anti-PD-1/PD-L1 does not seem to induce changes in the immune compartment of non-inflamed organs.[7 46] While scRNA-seq and scTCR-seq data allowed us to put forward several interesting mechanistic hypotheses, further research is needed to validate these hypotheses. Finally, our data cannot provide an answer to the question why some patients develop ICI-pneumonitis and others do not. Indeed, while we provide data on the TCR repertoire in ICI-pneumonitis BALF, larger studies combining in-silico TCR repertoire with in vitro TCR reactivity data (examining (cross-)reactivity of T cells in ICI-pneumonitis lesions) are presumably key to identify the substrate of the immune reaction in ICI-pneumonitis. In parallel, genomic studies (eg, examining IL-23R or IL-10R polymorphisms) will help to uncover susceptibility factors to the development of irAEs.[47]

In conclusion, we use scRNA-seq and scTCR-seq to perform a deep immune profiling effort and characterize the immune response in ICI-pneumonitis, thereby yielding novel pathophysiological insights. We offer a clear rationale for a novel targeted treatment approach for ICI-pneumonitis to improve outcome of this potentially fatal irAE while maintaining tumor control.

Author affiliations
[1]VIB - CCB Department of Human Genetics, KU Leuven, Leuven, Flemish Brabant, Belgium
[2]Pneumology - Respiratory Oncology, Katholieke Universiteit Leuven Universitaire Ziekenhuizen Leuven, Leuven, Flemish Brabant, Belgium
[3]Department of Chronic Diseases and Metabolism, KU Leuven, Leuven, Flemish Brabant, Belgium
[4]Pneumology, Katholieke Universiteit Leuven Universitaire Ziekenhuizen Leuven, Leuven, Flemish Brabant, Belgium
[5]Department of Imaging & Pathology, KU Leuven, Leuven, Flemish Brabant, Belgium
[6]Department of Microbiology, Immunology and Transplantation, KU Leuven, Leuven, Flemish Brabant, Belgium

Twitter Amelie Franken @ameliefranken and Els Wauters @ewauters

Acknowledgements We acknowledge the massive effort of all patients, researchers (PhDs/postdocs), clinicians and nurses involved.

Contributors AF contributed to methodology and performed formal analysis, visualization, investigation and writing (original draft and revision). PVM contributed to methodology and project administration, formal analysis, investigation, resource gathering and data curation and performed writing (original draft and revision). SV and ED contributed to investigation and provided resources. RS and TVB performed experiments. CD, JY, NDC, DT, WDW, KN, JV, RV and SH-B provided resources and performed investigation. DL and EW conceptualized the study, provided resources, performed investigation and writing (original draft and revision), supervised the study, and were responsible for project administration and funding acquisition. EW accepts responsibility for the work as guarantor.

Funding This work was supported by internal KU Leuven (Belgium) and UZ Leuven (Belgium) funding. This project has received funding from Foundation against Cancer, Flemish Fund for Scientific Research (FWO; projects G0B6120N and G065615N). AF is supported by a Stand up to Cancer research fund. PVM is supported by an FWO PhD fellowship (1S66020N). RV and JV are supported by an FWO Fundamental Clinical Mandate (1803521N and 1833317N, respectively). EW is supported by the Belgian Foundation against Cancer (Mandate for basic & clinical oncology research). PVM, JV and EW acknowledge the patronage of the KU Leuven M.D. Davidse Research Chair for Immuno-oncological Research.

Competing interests None declared.

Patient consent for publication Not applicable.

Ethics approval Ethical approval was obtained from the Research Ethics Committee of KU / UZ Leuven (S63357). Participants gave informed consent to participate in the study before taking part.

Provenance and peer review Not commissioned; externally peer reviewed.

Data availability statement Data are available in a public, open access repository. Raw sequencing reads of the scRNA-seq and scTCR-seq experiments generated for this study will be deposited in the EGA European Genome-Phenome Archive database upon publication. The publicly available data sets that supported this study are available from ArrayExpress under accessions E-MTAB-6149 and E-MTAB-6653.

ORCID iDs
Amelie Franken http://orcid.org/0000-0003-4121-4016
Els Wauters http://orcid.org/0000-0002-0115-0030

REFERENCES

1 Waldman AD, Fritz JM, Lenardo MJ. A guide to cancer immunotherapy: from T cell basic science to clinical practice. *Nat Rev Immunol* 2020;20:651–68.
2 Haanen JBAG, Carbonnel F, Robert C, *et al*. Management of toxicities from immunotherapy: ESMO clinical practice guidelines for diagnosis, treatment and follow-up. *Ann Oncol* 2017;28:iv119–42.
3 Suresh K, Voong KR, Shankar B, *et al*. Pneumonitis in non-small cell lung cancer patients receiving immune checkpoint immunotherapy: incidence and risk factors. *J Thorac Oncol* 2018;13:1930–9.
4 Wang DY, Salem J-E, Cohen JV, *et al*. Fatal toxic effects associated with immune checkpoint inhibitors: a systematic review and meta-analysis. *JAMA Oncol* 2018;4:1721–8.
5 Reynolds KL, Arora S, Elayavilli RK, *et al*. Immune-Related adverse events associated with immune checkpoint inhibitors: a call to action for collecting and sharing clinical trial and real-world data. *J Immunother Cancer* 2021;9:e002896.
6 Naing A, Hajjar J, Gulley JL, *et al*. Strategies for improving the management of immune-related adverse events. *J Immunother Cancer* 2020;8:e001754.
7 Suresh K, Naidoo J, Zhong Q, *et al*. The alveolar immune cell landscape is dysregulated in checkpoint inhibitor pneumonitis. *J Clin Invest* 2019;129:4305–15.
8 Wang YN, Lou DF, Li DY, *et al*. Elevated levels of IL-17A and IL-35 in plasma and bronchoalveolar lavage fluid are associated with checkpoint inhibitor pneumonitis in patients with non-small cell lung cancer. *Oncol Lett* 2020;20:611–22.
9 Lin X, Deng J, Deng H, *et al*. Comprehensive analysis of the immune microenvironment in checkpoint inhibitor pneumonitis. *Front Immunol* 2021;12:818492.
10 Tanaka R, Ichimura Y, Kubota N, *et al*. Activation of CD8 T cells accelerates anti-PD-1 antibody-induced psoriasis-like dermatitis through IL-6. *Commun Biol* 2020;3:571.
11 Läubli H, Koelzer VH, Matter MS, *et al*. The T cell repertoire in tumors overlaps with pulmonary inflammatory lesions in patients treated with checkpoint inhibitors. *Oncoimmunology* 2018;7:e1386362.
12 Hao Y, Hao S, Andersen-Nissen E, *et al*. Integrated analysis of multimodal single-cell data. *Cell* 2021;184:e29:3573–87
13 Lambrechts D, Wauters E, Boeckx B, *et al*. Phenotype molding of stromal cells in the lung tumor microenvironment. *Nat Med* 2018;24:1277–89.
14 Qian J, Olbrecht S, Boeckx B, *et al*. A pan-cancer blueprint of the heterogeneous tumor microenvironment revealed by single-cell profiling. *Cell Res* 2020;30:745–62.
15 Aversa I, Malanga D, Fiume G, *et al*. Molecular T-cell repertoire analysis as source of prognostic and predictive biomarkers for checkpoint blockade immunotherapy. *Int J Mol Sci* 2020;21. doi:10.3390/ijms21072378. [Epub ahead of print: 30 Mar 2020].
16 Signorell A. *DescTools: tools for descriptive statistics. R package version 0.99.45*, 2022.
17 Lange M, Bergen V, Klein M, *et al*. CellRank for directed single-cell fate mapping. *Nat Methods* 2022;19:159–70.
18 Roncarolo MG, Gregori S, Bacchetta R, *et al*. The biology of T regulatory type 1 cells and their therapeutic application in immune-mediated diseases. *Immunity* 2018;49:1004–19.
19 Ingelfinger F, De Feo D, Becher B. Gm-Csf: master regulator of the T cell-phagocyte interface during inflammation. *Semin Immunol* 2021;54:101518.
20 Kaiser Y, Lepzien R, Kullberg S, *et al*. Expanded lung T-bet+RORγT+ CD4+ T-cells in sarcoidosis patients with a favourable disease phenotype. *Eur Respir J* 2016;48:484–94.
21 Harbour SN, Maynard CL, Zindl CL, *et al*. Th17 cells give rise to Th1 cells that are required for the pathogenesis of colitis. *Proc Natl Acad Sci U S A* 2015;112:7061–6.
22 Gagliani N, Amezcua Vesely MC, Iseppon A, *et al*. Th17 cells transdifferentiate into regulatory T cells during resolution of inflammation. *Nature* 2015;523:221–5.
23 Ogishi M, Yang R, Aytekin C, *et al*. Inherited PD-1 deficiency underlies tuberculosis and autoimmunity in a child. *Nat Med* 2021;27:1646–54.
24 Voskoboinik I, Whisstock JC, Trapani JA. Perforin and granzymes: function, dysfunction and human pathology. *Nat Rev Immunol* 2015;15:388–400.
25 Wang H, Zhou F, Zhao C, *et al*. Interleukin-10 is a promising marker for immune-related adverse events in patients with non-small cell lung cancer receiving immunotherapy. *Front Immunol* 2022;13:840313.
26 McCallen JD, Naqash AR, Marie MA, *et al*. Peripheral blood interleukin 6, interleukin 10, and T lymphocyte levels are associated with checkpoint inhibitor induced pneumonitis: a case report. *Acta Oncol* 2021;60:813–7.

27 Ohkura N, Sakaguchi S. Transcriptional and epigenetic basis of Treg cell development and function: its genetic anomalies or variations in autoimmune diseases. *Cell Res* 2020;30:465–74.
28 Guo B. Il-10 modulates Th17 pathogenicity during autoimmune diseases. *J Clin Cell Immunol* 2016;7. doi:10.4172/2155-9899.1000400. [Epub ahead of print: 22 03 2016].
29 Kishi Y, Kondo T, Xiao S, *et al*. Protein C receptor (PROCR) is a negative regulator of Th17 pathogenicity. *J Exp Med* 2016;213:2489–501.
30 Gaublomme JT, Yosef N, Lee Y, *et al*. Single-Cell genomics unveils critical regulators of Th17 cell pathogenicity. *Cell* 2015;163:1400–12.
31 Ichiyama K, Gonzalez-Martin A, Kim B-S, *et al*. The MicroRNA-183-96-182 cluster promotes T helper 17 cell pathogenicity by negatively regulating transcription factor FoxO1 expression. *Immunity* 2016;44:1284–98.
32 Jain R, Chen Y, Kanno Y, *et al*. Interleukin-23-Induced transcription factor Blimp-1 promotes pathogenicity of T helper 17 cells. *Immunity* 2016;44:131–42.
33 Stadhouders R, Lubberts E, Hendriks RW. A cellular and molecular view of T helper 17 cell plasticity in autoimmunity. *J Autoimmun* 2018;87:1–15.
34 Nikitina IY, Panteleev AV, Kosmiadi GA, *et al*. Th1, Th17, and Th1Th17 Lymphocytes during Tuberculosis: Th1 Lymphocytes Predominate and Appear as Low^{-}Differentiated $CXCR3^{+}CCR6^{+}$ Cells in the Blood and Highly Differentiated $CXCR3^{+/-}CCR6^{-}$ Cells in the Lungs. *J Immunol* 2018;200:2090–103.
35 Meyer KC, Raghu G, Baughman RP, *et al*. An official American thoracic Society clinical practice guideline: the clinical utility of bronchoalveolar lavage cellular analysis in interstitial lung disease. *Am J Respir Crit Care Med* 2012;185:1004–14.
36 El-Behi M, Ciric B, Dai H, *et al*. The encephalitogenicity of T(H)17 cells is dependent on IL-1- and IL-23-induced production of the cytokine GM-CSF. *Nat Immunol* 2011;12:568–75.
37 Lim SY, Lee JH, Gide TN, *et al*. Circulating cytokines predict immune-related toxicity in melanoma patients receiving Anti-PD-1-Based immunotherapy. *Clin Cancer Res* 2019;25:1557–63.
38 Metzemaekers M, Vanheule V, Janssens R, *et al*. Overview of the mechanisms that may contribute to the non-redundant activities of interferon-inducible CXC chemokine receptor 3 ligands. *Front Immunol* 2017;8:1970.
39 Schutyser E, Struyf S, Van Damme J. The CC chemokine CCL20 and its receptor CCR6. *Cytokine Growth Factor Rev* 2003;14:409–26.
40 Khan S, Khan SA, Luo X, *et al*. Immune dysregulation in cancer patients developing immune-related adverse events. *Br J Cancer* 2019;120:63–8.
41 Sakuraba A, Sato T, Kamada N, *et al*. Th1/Th17 immune response is induced by mesenteric lymph node dendritic cells in Crohn's disease. *Gastroenterology* 2009;137:1736–45.
42 Suresh K, Naidoo J, Lin CT, *et al*. Immune checkpoint immunotherapy for non-small cell lung cancer: benefits and pulmonary toxicities. *Chest* 2018;154:1416–23.
43 Das S, Johnson DB. Immune-Related adverse events and anti-tumor efficacy of immune checkpoint inhibitors. *J Immunother Cancer* 2019;7:306.
44 Zhan Y, Lew AM, Chopin M. The pleiotropic effects of the GM-CSF rheostat on myeloid cell differentiation and function: more than a numbers game. *Front Immunol* 2019;10:2679.
45 Esfahani K, Elkrief A, Calabrese C, *et al*. Moving towards personalized treatments of immune-related adverse events. *Nat Rev Clin Oncol* 2020;17:504–15.
46 Thomas MF, Slowikowski K, Manakongtreecheep K, *et al*. Altered interactions between circulating and tissue-resident CD8 T cells with the colonic mucosa define colitis associated with immune checkpoint inhibitors. *BioRxiv* 2021.
47 Weidhaas J, Marco N, Scheffler AW, *et al*. Germline biomarkers predict toxicity to anti-PD1/PDL1 checkpoint therapy. *J Immunother Cancer* 2022;10:e003625.